Hindawi
Advances in Materials Science and Engineering
Volume 2019, Article ID 8674323, 13 pages
https://doi.org/10.1155/2019/8674323

Research Article

Effect of Isothermal Treatment on Microstructure and Mechanical Properties of Cold-Deformed IF Steel

Jose Luis Reyes Barragan,[1] **Roberto Ademar Rodriguez Diaz**,[2] **Maria Luisa Ojeda Martinez**,[1] **Silvia Gaona Jimenez**,[3] **and Julio Alberto Juarez Islas**[4]

[1]*Research Centre of Nanoscience and Nanotechnology – Guadalajara University, Jalisco 46600, Mexico*
[2]*Technologic of Superior Studies of Coacalco, Subdirection of Professional Studies "A", Coacalco de Berriozábal 55700, Mexico*
[3]*Polytechnic University of Morelos State, Jiutepec 62574, Mexico*
[4]*Materials-Research Institute, National University Autonomous of Mexico, Coyoacán 04510, Mexico*

Correspondence should be addressed to Roberto Ademar Rodriguez Diaz; german.rodericus@gmail.com

Received 27 August 2018; Revised 19 November 2018; Accepted 17 January 2019; Published 12 March 2019

Academic Editor: Pavel Lejcek

In this study, we investigated the recrystallisation kinetics of Ti-stabilised interstitial-free (IF) steel manufactured by the Mexican steel industry through the route of electric arc furnace with vacuum degassing, secondary refining, and subsequent continuous casting. The IF steel was hot-rolled at 950°C and then cold-rolled until deformation of 94% was attained, followed by recrystallisation at different times at a constant temperature of 780°C. In addition, the mechanical properties of the IF steel were assessed as a function of recrystallisation time. The results obtained from the mechanical property tests were presented in the form of plots of microhardness, yield strength, ultimate tensile stress, and deformation percent as functions of the recrystallised fraction with an indirect dependence on recrystallisation time. A graphical model of the recrystallisation behaviour showed the evolution of the microstructure, including phase transformations, hardness, and the mechanical properties determined from the tensile tests. In view of subsequent recovery and recrystallisation, stored energy analysis derived from the strain induced by deformation was presented. Furthermore, we determined the precipitates formed in the different processing stages of IF steel.

1. Introduction

The Mexican steel industry is presently introducing new products or improving existing ones, to reduce C content to less than 0.02%, to ensure compliance with global standards for the manufacture of automotive sheet and its stampability [1, 2].

The utilisation of special steels suited for applications in the automotive industry has grown drastically over the last few decades. Their applications can be classified into two major categories: body panels and body-in-white parts. In the case of outer body panels, the main driving force has been the continuous research into fuel economy and, hence, weight reduction. This implies the use of more formable steels for the manufacture of intricate design parts as well as part consolidation. Additionally, the diminution of the gauges for weight conservation has led to the utilisation of high-strength interstitial-free (IF) and bake-hardened IF steel [3]. Typically, IF mild steel has an ultralow level of C concentration (commonly less than 50 parts per million (ppm)). Its entire C and N contents exist in combination with elements such as Ti and Nb that form nitrides and carbides. Steels with these microstructural features thus have low yield strengths and high elongations, n-values, and r-values. Based on this premise, IF steel has been employed in mild steel parts that require enhanced formability [4].

Several types of research have been conducted on the recovery and recrystallisation behaviour of IF steel. Some of these investigations have focused on the effects of recrystallisation time and temperature of previously deformed

specimens on their microstructures and mechanical behaviours. The study of recovery and recrystallisation behaviour has been conducted via electromagnetic characterisation, electron backscatter diffraction (EBSD), hardness tests, and adaptive criteria. To investigate the influence of processing methods on subsequent recrystallisation behaviour, several studies have focused on manufacturing IF steel through various processes such as severe deformation, differential speed rolling (DSR), and equal channel angular extrusion (ECAE) among others.

Qiu et al. studied the microstructure and mechanical properties of hot-rolled IF steel annealed at four different temperatures (730°C, 760°C, 790°C, and 820°C) [5]. The authors determined that when the annealing temperature was increased from 730°C to 820°C, the yield strength and ultimate tensile strength declined while elongation simultaneously increased from 44% to 49.6%.

Sekban et al. studied the microstructure, mechanical properties, and stretch formability of fine-grain IF steel formed by friction stir processing (FSP) [6]. The authors reported that one-pass FSP induced a drastic refinement of the microstructure by the mechanism of dynamic recrystallisation. The authors established that coarse-grain (CG) specimens exhibited high formability and deformed uniformly under biaxial strain loading conditions. Grain refinement induced by FSP had no significant effect on stretch formability and deformation behaviour under biaxial tension loading conditions.

Saray et al. studied the impact toughness of ultrafine-grain (UFG) IF steel fabricated by ECAE/pressing (ECAE/P) at room temperature [7]. The authors stated that UFG IF steel displayed an improved combination of strength and impact toughness when compared with its CG counterpart. Grain refinement by multipass ECAE enhanced toughness by increasing the upper-shelf energy and lower-shelf energy and decreasing the ductile-brittle transition temperature.

Roy et al. assessed the recovery and recrystallisation behaviour of cold-rolled IF steel through nondestructive electromagnetic characterisation and hardness tests [8]. The authors reported that nucleation of new, recrystallised grains was observed in the specimen annealed at 600°C/15 min, while completion of recrystallisation was achieved in the specimen annealed at 700°C/15 min. Moreover, the decrease in dislocation density during the initial stage of annealing ($T < 550$°C) induced a lowering of coercivity and an increment in the number of low-amplitude magnetic Barkhausen emission pulses. The results derived from the research of Roy et al. suggest that it is more effective to employ the technique of electromagnetic characterisation to measure the progress of recovery [8].

Dziaszyk et al. studied the recrystallised fraction of Ti-stabilised IF steel by optical metallography, EBSD, and hardness-based techniques [9]. The results of the research indicate that misorientation-based techniques, when meticulously implemented, may be utilised to adequately determine the recrystallisation fraction. Moreover, the nanohardness results illustrate the variations in mechanical properties that are developed among individual grains with recrystallisation. The recrystallisation kinetics determined by different techniques may vary based on the EBSD analysis methodology utilised.

Suharto et al. studied the annealing behaviour of severely deformed IF steel processed by DSR, and the total reduction in sample thickness was 75% [10]. The severely deformed specimens were subjected to heat treatments at various temperatures in the range 400–650°C at intervals of 50 degrees (Celsius) for 1 h each. The authors reported that the specimen obtained via four-pass DSR displayed the highest microhardness value, and this was attributable to UFGs and high dislocation density. At temperatures under 550°C, the microhardness values of the annealed samples decreased due to the rearrangement and annihilation of dislocations, and this interval of temperature was dominated by static recovery. Recrystallisation was clearly observed after annealing at 550°C, while grain growth appeared after annealing at temperatures above 600°C [11, 12].

Song et al. performed annealing treatments at 810°C on cold-rolled (75% reduction ratio) Ti-IF steel, and evaluated the influence of the annealing parameters on the microstructure, mechanical properties, and phosphorus segregation at grain boundaries [13]. The research results revealed that recrystallisation concluded after annealing at 810°C for 180 s. The tensile strength and yield strength decreased as annealing time increased.

Kim et al. proposed a method to characterise the microstructure evolution during annealing of IF steel, cold-rolled to strain levels of 0.7 and 1.6 [14]. The recrystallisation kinetics determined by EBSD using an adaptive criterion was found to be consistent with those obtained from the standard method of Vickers microhardness test. The specimen previously deformed at room temperature was isothermally annealed at various temperatures in the range 500–800°C for 1 h. The authors determined that microhardness diminished with increase in recrystallisation temperature.

Saray et al. performed annealing treatments on UFG IF steel processed by ECAE. The authors reported that annealing increased the ductility and formability of UFG steel [15]. In addition, the annealing temperature within the recovery regime promoted a limited enhancement of the formability of UFG steel due to the release of internal energy. The yield strength and ultimate tensile strength exhibited by UFG IF steel were considerably higher than those of CG IF steel; however, the ductility of CG IF steel was lower than that of UFG IF steel.

Saray et al. studied the stretch formability of UFG IF steel processed by ECAE/P [16]. A CG specimen revealed high formability with an Erichsen Index of 4.5 mm. The microstructure refinement induced by ECAE/P reduced the formability but increased the required punch load depending on the applied strain paths. The authors reported significant increases in the yield strength and ultimate tensile strength of the UFG IF steel following ECAE/P. This behaviour can be attributed to the significant grain refinement (Hall–Petch effect) and stored dislocations (dislocation hardening) formed [17, 18].

There is evidently a lack of research focused on the development of a model to describe the evolution of microstructure, mechanical properties, precipitation

behaviour, and variation in the stored energy derived from the transformation from deformed state to subsequent recovery and recrystallisation of microstructures in IF steel subjected to isothermal annealing.

In this work, the evolution of microstructure, mechanical properties, precipitation behaviour, and analysis of stored energy are presented by adopting a synthesized model that facilitates the determination of relationships between the isothermal annealing time and the recrystallised fraction, dislocation density, and energy stored and its influence on the mechanical behaviour and microstructural properties of IF steel.

2. Materials and Methods

2.1. Processing of IF Steel. Continuously cast steel ingots were cut into small pieces of the following dimensions: thickness of 3 cm, width of 8 cm, and length of 21 cm. The chemical compositions of these samples were determined by optical emission spectroscopy, and the results are presented in Table 1. The samples were rolled at 950°C (above Ar_3) and at a speed of 3.3 rpm with a reduction in thickness of 0.8 mm at each stage until a final deformation of 66% was attained. Following hot-rolling, the samples were cold-rolled at the same speed, and a deformation percent of 94% was attained. The specimens were then annealed at 780°C for the following durations: 0, 60, 120, 180, 240, 300, 360, and 420 s. The resultant samples were cold-rolled to a thickness of 0.5 mm. They were subsequently annealed at 780°C for different durations: 0, 60, 120, 180, 240, 300, 360, and 420 s.

2.2. Metallographic Preparation of Samples. The steel samples of $1.0 \times 1.0\,cm^2$ were mounted on polyester resin. The surfaces on which microstructural characterisation was to be performed were prepared by sequential grinding with SiC paper up to #2000 finishing. The samples were then mechanically polished using 1 μm alumina slurry. In the final stage of sample preparation, the specimens were etched with Nital 2% to reveal the microstructure.

2.3. Microstructural Characterisation of Samples. The microstructural characteristics of some specimens were studied using scanning electron microscopy (SEM, JEOL JSM-5900 LV). In addition, transmission electron microscopy (TEM) was employed to characterise and determine the morphology and types of precipitates of a few specific samples. For these analyses, a transmission electron microscope (JEOL model T120) operating at 120 kV was utilised. The specimens, 3 mm in diameter and 50 μm in thickness, were perforated using a Struers electrolytic thinning equipment. An electrolytic solution comprising 5 mL of $HClO_4$ in 95 mL of CH_3CH_2OH was utilised to perforate the samples at a temperature of –10°C and a voltage of 25 V. The recrystallised grain sizes of the processed specimens were determined in accordance with the methods described in ASTM E112 [19].

2.4. Characterisation of Mechanical Properties. The tension specimens were machined according to the method described in ASTM E8 for flat specimens, and the tension tests were performed on a 20 t MTS machine with a displacement speed of 1 mm/min [20].

The Vickers microhardness values were determined using a Shimadzu microhardness tester with an applied load of HV 0.2 (1,961 N) and indentation time of 10 s. The mean hardness value was determined from 10 measurements.

3. Results and Discussion

3.1. Microstructural Evolution during Isothermal Annealing of IF Steel

3.1.1. Characterisation of Microstructural Evolution by SEM. The initial grain size of IF steel, hot-rolled at 950°C, was 28 μm. It is noteworthy that the grain size decreased significantly following recrystallisation, which led to the formation of new grains with sizes in the range 14–16 μm (see Figure 1).

Figure 1 exhibits the microstructural evolution of hot-rolled IF steel as a function of the duration of recrystallisation performed at 780°C. It can be seen from this set of micrographs that the onset of recrystallisation took place at 180 s with the smaller new grains appearing on the deformed microstructure during the first 60–120 s of the thermal treatment, and a typical deformed grain morphology can be observed. Thus, the recovery of the deformed state took place during the first 60–120 s. In this case, the recovery mode is static; this is because the IF steel was cold-rolled at room temperature since dynamic recovery generally proceeds when steel is deformed at high temperatures. Additionally, Figures 1(d) and 1(e) exhibit that during these periods of the thermal treatment, "nucleation" or initiation of recrystallisation had taken place along with growth of the newly "nucleated" grains. In addition, from 300 to 420 s, the recrystallised fraction of the material advanced until the process concluded.

The mean grain size was determined for the samples subjected to recrystallisation for 240–420 s. Figure 1(a) shows that a highly deformed grain microstructure was obtained after cold deformation. Under this processing condition, the stored energy of the deformed grains, which constitutes the driving force of recrystallisation, is higher. It is noteworthy that during the first 180 s of thermal treatment, the microstructure consisted predominantly of greatly deformed grains.

Table 2 displays the variation in grain size as a function of recrystallisation time. The grain size increased from 2.56 μm at 60 s to 17.1 μm at 400 s of the thermal treatment. According to Figure 2, the process of recovery was predominant in the first 180 s of annealing; the recrystallised grains began to nucleate during the first 60–180 s of treatment, and the grains underwent continuous growth from 2.56 μm to 8.0 μm in this time interval. However, after 180 s, the microhardness curve as a function of annealing time exhibited an increment in slope, which prevailed from 180 s to about 360 s. This behaviour is associated with the prevalence of recrystallisation,

Table 1: Chemical composition of IF steel.

	Fe	C	Mn	Si	P	S	Al	Ti	Cu	Cr	Mo	Ni	N	Co
wt.%	Bal	0.003	0.145	0.030	0.017	0.015	0.016	0.100	0.044	0.013	0.070	0.013	0.005	0.002

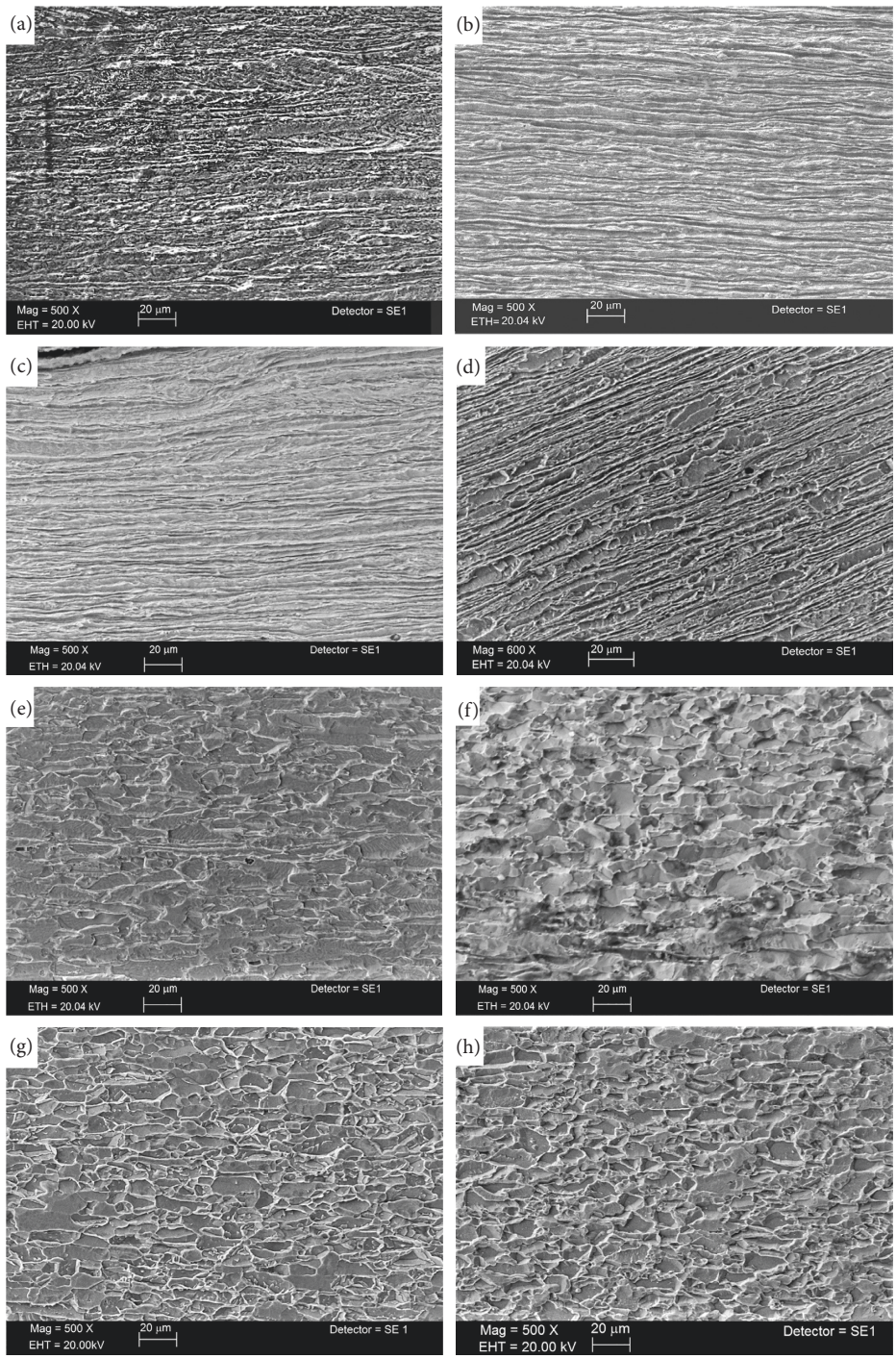

Figure 1: Scanning electron micrographs (SEM images) showing the effect of recrystallisation treatment at 780°C on the microstructural evolution of cold-rolled IF steel at different times. (a) 0 s, (b) 60 s, (c) 120 s, (d) 180 s, (e) 240 s, (f) 300 s, (g) 360 s, and (h) 420 s.

and the grain size rose from 8 μm to 15.2 μm during this interval of time.

It is noteworthy that the deformation percent before annealing considerably influences the recrystallised grain size. Saha performed a systematic study on the evolution of microstructure of an industrially elaborated IF steel following severe deformation of 90% and 98% by cold rolling with subsequent recrystallisation annealing [21].

Table 2: Mechanical properties of IF steel as a function of recrystallisation time.

Recrystallisation treatment time (s)	Young's modulus, E (GPa)	Yield strength, Y_c (MPa)	Ultimate tensile strength, UTS (MPa)	Deformation percent, e (%)	Grain size (μm)
0	58.7 ± 2	426 ± 3	613 ± 3	3 ± 0.1	—
60	55.9 ± 2	364 ± 3	527 ± 3	5.3 ± 0.1	2.5 ± 0.1
120	74 ± 2	342 ± 3	425.5 ± 3	13.9 ± 0.1	4.9 ± 0.1
180	111 ± 2	147.4 ± 3	327.3 ± 3	32.8 ± 0.1	8.0 ± 0.1
240	132 ± 2	157 ± 3	341 ± 3	37.4 ± 0.1	10.8 ± 0.1
300	28.6 ± 2	130 ± 3	316 ± 3	45.6 ± 0.1	11.9 ± 0.1
360	47.6 ± 2	120 ± 3	310 ± 3	48.2 ± 0.1	15.2 ± 0.1
420	63.5 ± 2	108.4 ± 3	294 ± 3	52 ± 0.1	17.1 ± 0.1

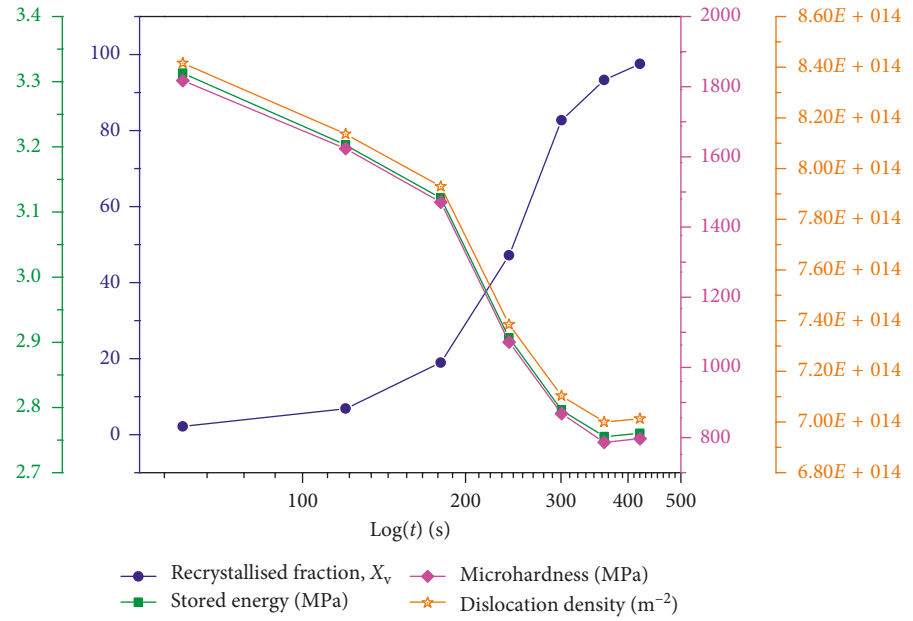

Figure 2: Relationship of microhardness with recrystallised fraction, dislocation density, and stored energy of IF steel.

The authors determined that grain sizes were in the range 1–2 μm in the samples with 90% deformation that were annealed for 30 min as well as in the specimens with 98% deformation that were annealed for 45 min at 650°C.

3.1.2. Precipitation Behaviour on IF Steel. The content of C in typical IF steels is of an ultralow level (less than 50 ppm). In this case, N and C are combined with elements that form carbides and nitrides such as Ti and Nb [22]. The TEM image presented in Figure 3(a) shows the precipitates AlN/TiN and TiN. The presence of these precipitates corresponds to hot-rolled IF steel. It is noteworthy that the TiN precipitates are the biggest found in these steels regardless of their composition. The preferential sites for TiN precipitation are found to be mostly inside the grains. These precipitates were identified via energy dispersive X-ray (EDX) microanalysis performed on the surface of IF steels in this stage of processing (Figures 3(b) and 3(c)). It is noteworthy that precipitates smaller than 2 μm corresponded to TiN nitride, and those larger than 2 μm were identified as AlN/TiN.

The possible mechanisms of TiN precipitation are as follows:

(1) Direct combination of Ti and N atoms with subsequent growth

(2) Initial nucleation of Ti in AlN with subsequent growth

It is noteworthy that the characterisation performed by chemical mapping on TiN precipitates reveals the presence of TiN nucleates on the AlN particles previously formed. This behaviour can be represented by the chemical reactions presented in equations (1)–(3):

$$\mathrm{Al} + \mathrm{N} \longrightarrow \mathrm{AlN}\ (\text{steel deoxidation}) \quad (1)$$

$$\mathrm{N} + \mathrm{Ti} \longrightarrow \mathrm{TiN}\ (\text{steel stabilisation}) \quad (2)$$

$$\mathrm{AlN} + (\mathrm{TiN})\mathrm{Fe} \longrightarrow \mathrm{AlN/TiN}\ (\text{nucleation}) \quad (3)$$

It is well known that the process of precipitation in IF steel is a complex phenomenon. It has been reported that there are four main kinds of precipitates, i.e., TiN, TiS, $Ti_4C_2S_2$, and TiC, and the order of precipitation is $\mathrm{TiN} \longrightarrow \mathrm{TiS} \longrightarrow Ti_4C_2S_2 \longrightarrow \mathrm{TiC}$ [23].

A previous study related to the thermodynamics of precipitation reveals that the formation of TiN precipitates is favoured at temperatures above 900°C, while at temperatures

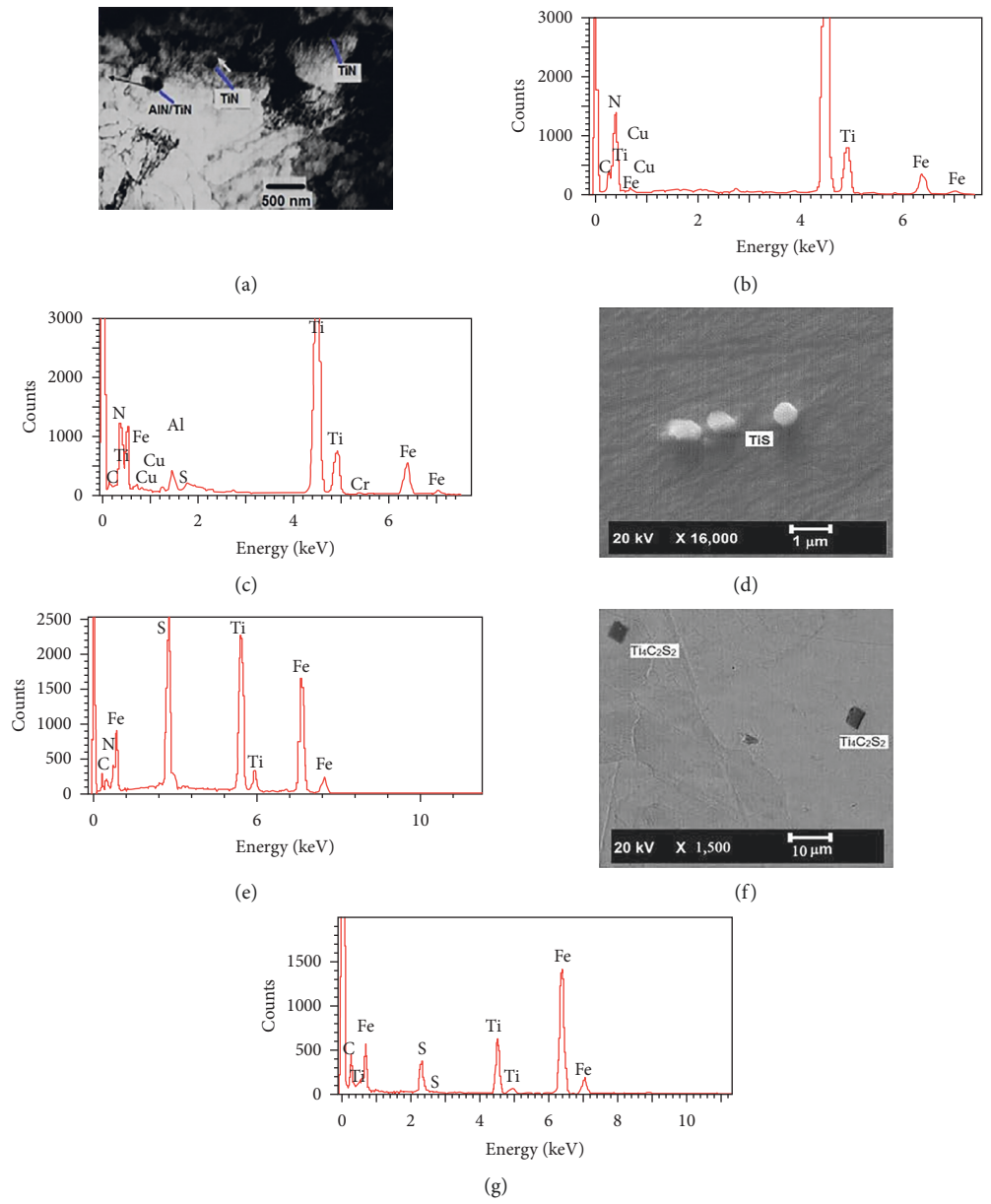

FIGURE 3: (a) Transmission electron micrographs (TEMs) showing precipitates with rhombohedral morphology (TiN), (b, c) EDX spectra of precipitates displayed, (d) SEM of TiS precipitates, (e) EDX spectra of TiS precipitates, (f) SEM of $Ti_4C_2S_2$ precipitates, and (g) EDX spectra corresponding to $Ti_4C_2S_2$ precipitates.

below 900°C, TiC precipitates gradually form and the content of these carbides increases with decrease in temperature [24]. Thus, the presence of TiN precipitates agrees with the temperature of formation of these nitrides, since IF steel was rolled at 950°C in the present work.

Also, Figure 3(d) exhibits round precipitates corresponding to TiS. This kind of precipitate has been observed in experimental steels. The morphology of these precipitates can change depending on the composition and processing techniques of steel, and these precipitates are often seen in the form of patches. These precipitates lie in the size range 200–500 nm [24]. The results derived from the chemical analyses are represented by the EDX spectra of TiS precipitates and are displayed in Figure 3(e).

Figure 3(f) also displays the presence of $Ti_4C_2S_2$, which possesses a rhombohedral form in hot-rolled IF steel. The chemical analysis based on the EDX technique denotes the presence of Ti, C, and S, which are associated with the formation of the $Ti_4C_2S_2$ precipitate (see Figure 3(g)). Thermodynamic computations firmly suggest the formation of these types of sulphides, and they have been considered as the main agents for C removal from solid solution [25]. The formation mechanism of this type of precipitate has been studied in previous investigations, and the authors of these works have stated that TiS transforms into $Ti_4C_2S_2$ by the mechanism of C diffusion [26, 27]. A schematic plot of the stability of different Ti compounds in IF steel as a function of precipitation

temperature was reported by Hua et al., and it was revealed that after the formation of TiN precipitates, TiS sulphides are likely to form as temperature decreases [28]. However, the stability of TiS is very low, and hence this sulphide decomposes during hot-rolling at 900–1200°C.

3.2. Recrystallisation Kinetics of Deformed IF Steel. The progress of recrystallisation as a function of thermal treatment time during isothermal annealing of IF steel at 780°C is displayed in Figure 4(a). This plot displays a typical sigmoidal morphology. It also exhibits an apparent incubation time from the beginning of thermal treatment up to around 60 s, an increment in recrystallisation rate at 180 s, a linear region from 180 s to 300 s, a decrease in the rate of recrystallisation from around 300 s to 400 s, and conclusion of recrystallisation at almost 400 s of heat treatment.

Humphreys et al. studied the primary recrystallisation of 70%, 80%, and 90% cold-rolled IF steel at temperatures in the range 590–675°C [29]. It is noteworthy that the recrystallisation kinetics plot determined by the authors at 630°C displays a considerably lower recrystallisation rate than that obtained in the present work for IF steel recrystallised at 780°C. This is because the annealing temperature has a profound effect on recrystallisation kinetics [30]. Besides, this statement agrees with equation (4) that expresses recrystallisation rate as a function of temperature.

$$\text{Rate} = \frac{1}{t_{0.5}} = C * \exp\left(-\frac{Q}{kT}\right), \tag{4}$$

where C and k are material constants, Q is the activation energy, T is the temperature, and $t_{0.5}$ is the required time for 50% of recrystallisation to take place.

Pereloma et al. studied the recrystallisation behaviour of IF steel during annealing [31]. Prior to recrystallisation, the steel was hot-rolled at 640°C and subsequently annealed at 700°C for durations in the range 10–2000 s. It is noteworthy that 50% of the recrystallised fraction was attained at about 600 s and complete recrystallisation at nearly 1000 s. These recrystallisation times are higher than those determined in the present work in which 50 % recrystallisation was achieved at about 260 s and complete recrystallisation at 450 s. This is because the relationship between recrystallisation rate and temperature is described or predicted by the Arrhenius equation.

The Johnson–Mehl–Avrami–Kolmogorov (JMAK) model, represented by equation (5), has been broadly utilised to describe the process of recrystallisation. Experimental recrystallisation kinetics data are typically compared with the JMAK model by plotting ln (–ln(1 – X)) as a function of ln(t). In accordance with equation (5), this should result in a straight line with a slope equal to the exponent n:

$$X_v = 1 - \exp\left(-kt^n\right). \tag{5}$$

The JMAK graph presents a curve with sigmoidal morphology (see Figure 4(a)), which is commonly seen in many transformation reactions and can be described phenomenologically in terms of the constituent nucleation and growth processes. Figure 4(b) depicts an approximately linear morphology [32–34].

3.3. Characterisation of the Evolution of Mechanical Properties

3.3.1. Variations in Hardness from Deformed to Recrystallised States. Microstructural variations that develop during recovery influence the mechanical behaviour of materials. Hence, recovery is generally measured in terms of the changes in the yield stress or hardness of the material although these changes are frequently small. Figure 2 shows the microhardness values as a function of time of recrystallisation performed at 780°C. In this graph, microhardness exhibits a diminishing trend from about 1800 MPa to 850 MPa with increase in recrystallisation time. Additionally, this plot reveals that microhardness diminished while the recrystallised fraction had progressed alongside a reduction in dislocation density (as determined from equation (6)), which is associated with the release of stored energy, as can be observed from Figure 2. Thus, static recovery induces a decrease in the internal stored energy by means of the rearrangement, reconfiguration, and removal of dislocations.

Besides, this plot exhibits a slope change in the curve of the variation in microhardness; the slope of the curve from 0 s to 180 s of annealing is lower than that from 180 s to 300 s. The small and continuous changes in hardness observed at the beginning of annealing are a characteristic of static recovery and are essentially due to the gradual decrease in the elastic distortion of the material, which is attributed to the decrease in the dislocation density, condensation, and annihilation owing to the formation of low-energy dislocation cell structures and the growth of these subgrains [29].

The higher slope observed in the time interval of 180–300 s is attributed to the development of the process of recrystallisation during this period. Under this regimen, the hardness decreases significantly and often at much higher rates than during recovery [35].

During recrystallisation, the original ductility possessed by the IF steel prior to cold deformation is restored, as can be seen from the enhancement of ductility as annealing progresses (see Figure 5) [36].

However, from 300 s to 420 s of heat treatment, the microhardness decreased slightly. This scarce softening of specimens is because recovery and recrystallisation were nearing completion. It is clear that from 0 s to 240 s of thermal treatment, hardness decreased at a higher rate than that in the final periods of recrystallisation. This behaviour is because the process of recovery was predominant in the first 240 s of the treatment (see Figures 1(a)–1(c)).

Urabe et al. performed cold-rolling reductions of 0.080/0Ti–0.01%Nb IF steel until reductions of 70% and 85% were achieved, following which the deformed samples were annealed at 720°C for various durations [37]. The authors reported a trend similar to that observed in the present work, i.e., the hardness diminished as recrystallisation progressed; despite this, the deformation percent was higher in the

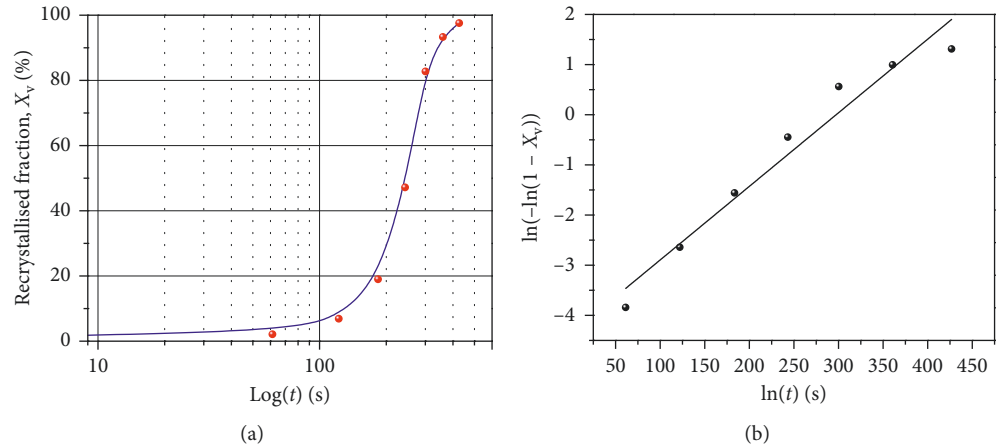

FIGURE 4: (a) Effect of recrystallisation kinetics for different isothermal annealing times of IF steel at 780°C, with 90% reduction, and (b) JMAK plot recrystallisation kinetics of IF steel at 780°C, with 90% reduction.

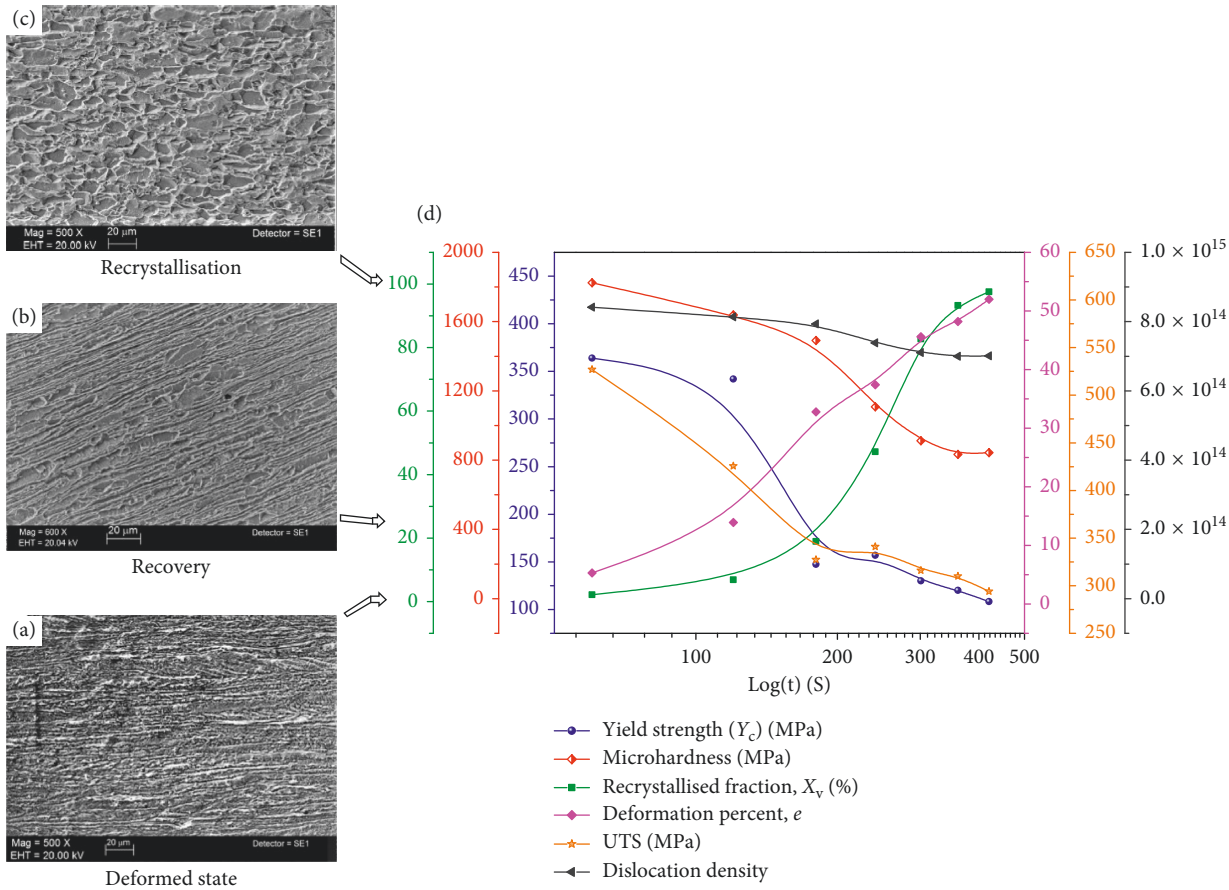

FIGURE 5: Model of the recrystallisation behaviour including the evolution of the microstructure and mechanical properties as functions of annealing time and the recrystallised fraction of IF steel.

present work. Additionally, the authors established that recrystallisation began after 10 s and 30 s of thermal treatment of the IF steel samples with 85% and 70% reduction, respectively.

Okuda et al. carried out hot-rolling in the ferrite region at various rolling temperatures and to achieve different rolling reductions [38]. This process was applied to IF steel with a composition of 0.016% Nb and 0.023% Ti. The hardness value changed from about 70 to 80 HV after heat treatment at 800°C and 850°C to about 118 HV after the specimens were hot-rolled at the same temperatures up to a reduction of 75%. In the present work, the values of hardness measured at 0 s, 60 s, and 120 s of annealing were superior, in the range 152–186 HV. This behaviour is certainly because the present

work entailed static recovery, whereas the cited work entailed a process of dynamic recovery; the former proceeds at a lower rate than the latter [38].

Kim et al. measured the variations in Vickers Hardness as a function of time of recrystallisation performed at 650°C of cold-rolled IF steel sheet [39]. The authors also reported a softening of the IF steel as the thermal treatment advanced. Additionally, the process of recrystallisation was accelerated after 5 min of annealing and concluded after 30 min of annealing.

Gazder et al. investigated the evolution of microhardness during recrystallisation treatment of an UFG IF steel processed by equal channel angular pressing followed by cold rolling to achieve a 95% reduction in thickness [40]. The authors revealed that microhardness decreased as recrystallisation progressed, and this trend is similar to that observed in the present work, since the values of deformation percent in both the cases were almost of the same order of magnitude.

Suharto et al. reported that the highest value of microhardness was achieved in an IF steel specimen subjected to severe deformation by means of DSR [10]; in this process, they obtained grain refinement from 35 μm to 0.7 μm and a microhardness value of 2300 MPa, which is higher than that achieved in the present work. This is due to the UFG size and the high dislocation density generated during the process of DSR. Additionally, the authors observed a decrease in hardness when the steel was annealed at temperatures lower than 500°C. The softening observed is similar to that seen in the present work and originated from the arrangement, reconfiguration, and removal of dislocations [11, 12]; this is in agreement with the tendency displayed by dislocation density (see Figure 2) [11].

The dislocation density of severely deformed IF steel was determined using equation (6) and based on the microhardness data associated with the internal stored energy after recrystallisation [41]:

$$\rho = \frac{1}{13.5}\left(\frac{H - H_0}{M \propto Gb}\right)^2, \tag{6}$$

where H_o is the microhardness of CG IF steel prior to cold deformation (~960 MPa), α is the geometric constant (~0.22), M is the Taylor factor of body-centred cubic metals (~3.08), G is the shear modulus of IF steel at room temperature (~64,000 MPa), and b is the Burgers vector (2.48×10^{-10} m) [42, 43].

Figure 2 shows the decreasing trend of dislocation density. Based on the results of annealing reported in a previous research, a diminution of the residual stress associated with the removal and rearrangement of dislocations was responsible for a decrease in the mechanical properties of the deformed mild steel, which is consistent with the present results [44].

A stored energy analysis was derived from the dislocation generated during strain derived from plastic deformation, and the subsequent release of stored energy because of removal or reconfiguration of dislocations was developed. The driving force of recrystallisation emerges from the removal of the dislocations introduced during cold deformation. The stored energy due to the dislocation density ρ is presented as

$$\xi = 0.5\rho G b^2, \tag{7}$$

where ξ is the stored energy (MPa), ρ is the dislocation density (m^{-2}), G is the shear modulus (MPa), and b (m) is the Burgers vector of dislocation. Figure 2 shows a plot of stored energy alongside dislocation removal or reconfiguration as a function of recrystallisation time. The plot displays that the stored energy is diminished as dislocation removal proceeds while the recrystallised fraction increases.

3.3.2. Characterisation of Tensile Mechanical Properties. Figures 6(a) and 6(b) show the stress deformation curves of IF steel subjected to recrystallisation for different durations. These plots clearly show that ductility increased as recrystallisation progressed. On the other hand, yield strength diminished as recrystallisation advanced. It is noteworthy that these trends are related to the competing processes of recovery and recrystallisation.

The deformation mode during mechanical tests does not induce any changes in the trends of variations in strength during recrystallisation. For example, in a previous research, the authors demonstrated that shear stress decreased as annealing at 525°C, 710°C, and 600°C progressed [28]. Furthermore, ductility decreased as recrystallisation advanced.

Table 2 shows the mechanical properties of IF steel as a function of recrystallisation time. Additionally, Figure 5(d) shows that ductility and recrystallised fraction increased alongside reductions in the dislocation density and stored energy associated with the presence of dislocations. This trend is associated with the process of recovery, which develops together with the annihilation and reconfiguration of dislocations into a lower-energy arrangement and nucleation and growth of new grains to produce polycrystalline steel.

Table 2 shows that the yield strength exhibited a declining trend but remained above 300 MPa during the first 120 s of thermal treatment. This decreasing tendency is clearly associated with the onset of recrystallisation, which is linked to a softening induced by the process of recovery during this interval. Moreover, the decrease in yield strength after this duration was more significant than that during the first 120 s of heat treatment. The yield strength also displays a predominant tendency to diminish during 180–400 s of recrystallisation. Besides, Figure 5(b) shows that the yield strength decreased while recrystallised fraction advanced progressively and that dislocation density diminished and is associated with release of stored energy. This phenomenon is explained in terms of the energy release promoted by the removal or reconfiguration of crystal defects such as vacancies and dislocations. In a previous research, IF steel sheets were processed by ECASE with subsequent annealing [45]. The processed sheets finally attained yield strength values of 463 MPa and 459 MPa. These values are higher than those obtained in the present work. This behaviour can be attributed to the deformation microstructure including refined subgrains with a high density of dislocations.

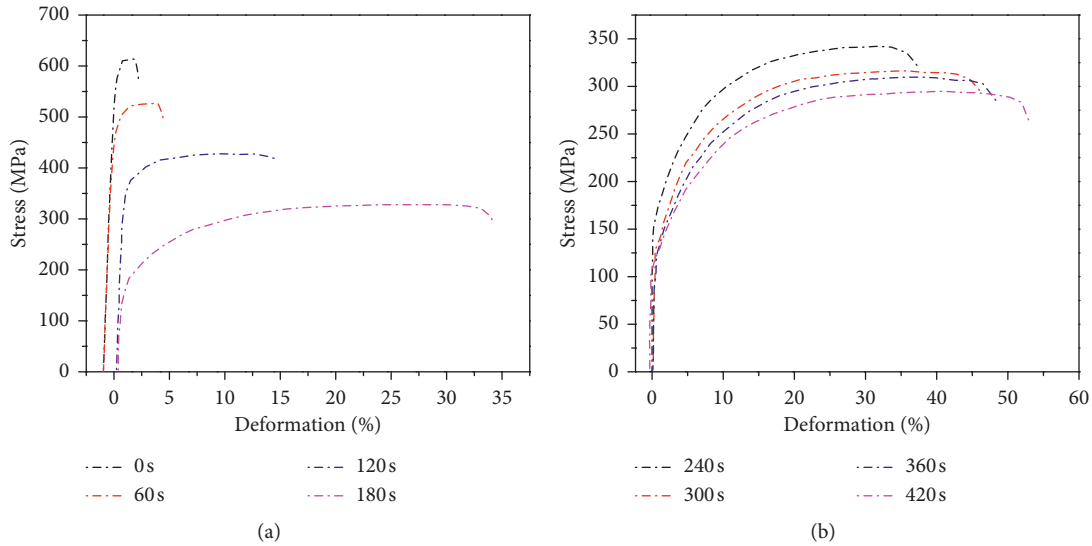

Figure 6: Stress-strain curves obtained for IF steel as a function of different recrystallisation times in the ranges (a) 0–180 s and (b) 240–420 s at a temperature of 780°C.

The ductility of IF steel, expressed in terms of deformation percent, exhibited a clear tendency to increase with recrystallisation. Figure 5(d) show that ductility enhanced progressively while recrystallised fraction also augmented. This trend is associated with the process of recovery, annihilation, and reconfiguration of dislocations, and nucleation and growth of new grains, which produce polycrystalline steel.

Other factors that could have contributed to the enhancement of ductility are grain refinement and production of a random crystallographic orientation of grains, which, in turn, favoured dislocation motion along the more randomly oriented slip crystal systems. It is noteworthy that ductility decreased alongside microhardness (see Figure 2). This behaviour is reasonable since ductility usually increases with progress in the softening of the material. Similarly, yield strength and microhardness diminished simultaneously. This behaviour is also associated with the softening induced by the processes of recovery and recrystallisation that occur during thermal treatment.

Saray et al. annealed UFG IF steel [45]. The processing technique of 8E ECAE induced a significant refinement of microstructure and transformed the CG microstructure (30 μm) into an UFG one (0.9 μm) with improved strength; the yield strength of CG steel was 106 MPa and that of UFG steel was 636 MPa, but ductility, expressed in terms of total elongation, decreased from 53% in CG IF steel to 16.4% in UFG steel. The higher value of yield strength obtained in the case of UFG steel when compared with those obtained in the present work (108–426 MPa) is due to the grain boundary strengthening in accordance with the Hall–Petch relation. Also, the ductility values of the UFG IF steel in the study cited are lower than the deformation percent obtained in present work (3–52%), and this is mainly due to the high dislocation density and elevated grain boundary surface produced by ECAE, which, in turn, induces a pinning effect in dislocation motion.

Furthermore, Figure 5(d) shows that the value of ultimate tensile strength tends to decrease as recrystallisation fraction increases and also highlights the removal and reconfiguration of these linear crystalline defects into a lower-energy configuration that is deduced by the diminution of stored energy (see Figure 2).

Table 2 shows that grain size exhibits a trend of continuous growth from the beginning to the end of annealing. It is noteworthy that these are recrystallised grains that had begun to grow from the deformed lamellar bands, which could belong to both γ and α fibres [46]. For example, Tong et al. studied the nucleation of cold-rolled IF steel in the early stages of recrystallisation [47]. The authors studied the deformed microstructure at 80% reduction. After deformation, two types of microstructures were identified: deformed bands bearing no crushed grains and deformed bands containing several crushed grains. The authors stated that the areas in which no grain or subgrain boundaries are visible belong to the α fibre orientation.

The reductions in yield strength and ultimate tensile strength as functions of recrystallisation time have also been reported previously. Song et al. performed annealing treatments at 810°C for different durations on a cold-rolled (75% reduction ratio) Ti-IF steel [13]. The authors also reported that both yield strength and ultimate tensile strength decreased during 180–600 s of annealing. In both cases, the behaviour is because the vacancies and dislocations annihilate and move towards the grain boundaries when the steel is subjected to recrystallisation annealing.

Purcek et al. severely deformed IF steel by ECAE/P and subsequently performed annealing at 600°C on the severely deformed sheets [48]. The authors investigated the effect of annealing time on the mechanical properties and reported that, in general, strength decreased while ductility increased progressively as annealing advanced. The behaviours observed in the present work and in the research cited stem

from the rapid microstructure recovery and the start of recrystallisation in some regions with high internal stresses. It has been well documented that severely deformed steels have the ability of fast recovery because the nonequilibrium subgrain boundaries contain high internal stresses [49]. Rapid recovery induces the annihilation and rearrangement of dislocations and polygonisation, with subsequent subgrain coalescence.

The observed variations in mechanical properties are principally a result of the change in the development of the recrystallised fraction of the microstructure as treatment progresses (see Figure 4). A few previous investigations have focused on the repercussion volume fraction of the recrystallised grains in terms of strength and ductility [50, 51]. These works have stated that yield strength diminishes whereas uniform elongation rises with increase in the volume fraction of recrystallised grains. Furthermore, both properties have an almost linear dependence on the volume fraction of recrystallised grains, suggesting that the rule of mixtures can be applied. It has been previously reported that the ultimate tensile strength and uniform elongation can be determined by applying the rule of mixtures [52].

4. Conclusions

In accordance with the model of recrystallisation developed in the present work to explain the evolution of the microstructure, involving phase transformations, hardness, and the mechanical properties, the main conclusions drawn are as follows.

Microhardness diminished with increase in annealing time and recrystallised fraction. Hardness decreased simultaneously, while the removal of dislocations proceeded together with their reconfiguration that occurred during static recovery and recrystallisation, and the development of these transformations, i.e., from the deformed state to the achievement of near-complete recrystallisation, was correlated to the release of stored energy.

Furthermore, ductility increased as annealing time advanced alongside a continuous increment in the recrystallised fraction. Despite the grain size decreasing during the first 360 s of annealing, the deformation percent diminished. This behaviour is mainly attributed to the removal and reconfiguration of dislocations, which are correlated with a diminution of the stored energy developed during static recovery and recrystallisation, and grain growth during 360–420 s of annealing.

When the IF steel was completely recrystallised, its ductility increased to that at about 50% deformation, which under these circumstances, renders the steel suitable for use in high-deformation process such rolling, forging, extrusion, and drawing.

During the microstructural characterisation of Ti-stabilised IF Steel, TiN, AlN/TiN, TiS, and $Ti_4C_2S_2$ precipitates were identified. The mechanisms proposed for TiN precipitation are direct combination of Ti and N atoms with subsequent growth or initial nucleation of Ti in AlN with subsequent growth. Additionally, it is proposed that TiS transforms into $Ti_4C_2S_2$ by the mechanism of C diffusion. In this work, TiS compound was precipitated during hot-rolling. However, the precipitate was formed within the temperature range 950–1100°C.

Additionally, the yield strength and ultimate tensile strength diminished simultaneously as annealing progressed, with growth in the recrystallised fraction following a similar trend. The diminution of strength and hardness with the continuous increase in ductility constitutes a typical behaviour of deformed materials during isothermal annealing and recrystallisation.

Data Availability

The data used to support the findings of this study are available from the corresponding author upon request.

Conflicts of Interest

The authors declare that there are no conflicts of interest regarding the publication of this paper.

Acknowledgments

This project was funded by "PROINPEP" and "NPP" and also by CONACYT, Mexico. The authors of this work express their gratitude to the Materials Research Institute, UNAM, for the use of its laboratories to develop the present project, as well as to the technician Adriana Tejeda for her support related to the microstructural characterisation of the samples. The authors also acknowledge PROINPEP which provided the economic resources to develop Project 243802 managed by the Academic Body of Sciences, Nanomaterials and Condensed Matter UDG-CA-583 and CONACYT for the scholarship provided to the Ph.D. student José Luis Reyes Barragan.

References

[1] I. F. Machado, "Technological advances in steels heat treatment," *Journal of materials processing technology*, vol. 172, no. 2, pp. 169–173, 2006.

[2] J. Ennis and A. Czyrska-Filemonowicz, "Recent advances in creep-resistant steels for power plant applications," *Sadhana*, vol. 28, no. 3-4, pp. 709–730, 2003.

[3] W. Cao, J. Shi, C. Wang et al., *The 3rd Generation Automobile Sheet Steels Presenting with Ultrahigh Strength and High Ductility. En Advanced Steels*, Springer, Berlin, Heidelberg, 2011.

[4] R. Pradhan, *Metallurgy of Vacuum-Degassed Steel Products*, TMS, Indianapolis, IN, USA, 1989.

[5] C.-y. Qiu, L. Li, L.-l. Hao, J.-g. Wang, X. Zhou, and Y.-l. Kang, "Effect of continuous annealing temperature on microstructure and properties of ferritic rolled interstitial-free steel," *International Journal of Minerals, Metallurgy, and Materials*, vol. 25, no. 5, pp. 536–546, 2018.

[6] D. M. Sekban, O. Saray, S. M. Aktarer, G. Purcek, and Z. Y. Ma, "Microstructure, mechanical properties and formability of friction stir processed interstitial-free steel,"

Materials Science and Engineering: A, vol. 642, pp. 57–64, 2015.

[7] O. Saray, G. Purcek, I. Karaman, and H. J. Maier, "Impact toughness of ultrafine-grained interstitial-free steel," *Metallurgical and Materials Transactions A*, vol. 43, no. 11, pp. 4320–4330, 2012.

[8] R. K. Roy, S. Dutta, A. K. Panda et al., "Assessment of recovery and recrystallisation behaviours of cold rolled IF steel through non-destructive electromagnetic characterisation," *Philosophical Magazine*, vol. 98, no. 21, pp. 1933–1944, 2018.

[9] S. Dziaszyk, E. J. Payton, F. Friedel, V. Marx, and G. Eggeler, "On the characterization of recrystallized fraction using electron backscatter diffraction: a direct comparison to local hardness in an IF steel using nanoindentation," *Materials Science and Engineering: A*, vol. 527, no. 29-30, pp. 7854–7864, 2010.

[10] J. Suharto and Y. G. Ko, "Annealing behavior of severely deformed IF steel via the differential speed rolling method," *Materials Science and Engineering: A*, vol. 558, pp. 90–94, 2012.

[11] B. Q. Han, F. A. Mohamed, and E. J. Lavernia, "Mechanical properties of iron processed by severe plastic deformation," *Metallurgical and Materials Transactions A*, vol. 34, no. 1, pp. 71–83, 2003.

[12] Y. Ding, J. Jiang, and A. Shan, "Microstructures and mechanical properties of commercial purity iron processed by asymmetric rolling," *Materials Science and Engineering: A*, vol. 509, no. 1-2, pp. 76–80, 2009.

[13] X. Song, Z. Yuan, J. Jia, D. Wang, P. Li, and Z. Deng, "Effect of phosphorus grain boundaries segregation and precipitations on mechanical properties for Ti-IF steel after recrystallization annealing," *Journal of Materials Science and Technology*, vol. 26, no. 9, pp. 793–797, 2010.

[14] D.-K. Kim, W.-W. Park, H. W. Lee, S.-H. Kang, and Y.-T. Im, "Adaptive characterization of recrystallization kinetics in IF steel by electron backscatter diffraction," *Journal of Microscopy*, vol. 252, no. 3, pp. 204–216, 2013.

[15] O. Saray, G. Purcek, I. Karaman, and H. J. Maier, "Improvement of formability of ultrafine-grained materials by post-SPD annealing," *Materials Science and Engineering: A*, vol. 619, pp. 119–128, 2014.

[16] O. Saray, G. Purcek, I. Karaman, and H. J. Maier, "Formability of ultrafine-grained interstitial-free steels," *Metallurgical and Materials Transactions A*, vol. 44, no. 9, pp. 4194–4206, 2013.

[17] A. A. Gazder, W. Cao, C. H. J. Davies, and E. V. Pereloma, "An EBSD investigation of interstitial-free steel subjected to equal channel angular extrusion," *Materials Science and Engineering: A*, vol. 497, no. 1-2, pp. 341–352, 2008.

[18] D. A. Hughes and N. Hansen, "Microstructure and strength of nickel at large strains," *Acta Materialia*, vol. 48, no. 11, pp. 2985–3004, 2000.

[19] ASTM International, ASTM E8/EM8, *Standard Test Methods for Determining Average Grain Size*, ASTM International, West Conshohocken, PA, USA, 2010.

[20] ASTM American Society for Testing and Materials, *Standard Test Methods for Tension Testing of Metallic Materials*, ASTM International, West Conshohocken, PA, USA, 2009.

[21] R. Saha and R. K. Ray, "Effect of severe cold rolling and annealing on the development of texture, microstructure and grain boundary character distribution in an interstitial free (IF) steel," *ISIJ International*, vol. 48, no. 7, pp. 976–983, 2008.

[22] J. Shi and X. Wang, "Comparison of precipitate behaviors in ultra-low carbon, titanium-stabilized interstitial free steel sheets under different annealing processes," *Journal of Materials Engineering and Performance*, vol. 8, no. 6, pp. 641–648, 1999.

[23] Y.-j. Hui, Y. Yu, L. Wang, C. Wang, W.-y. Li, and B. Chen, "Strain-induced precipitation in Ti micro-alloyed interstitial-free steel," *Journal of Iron and Steel Research International*, vol. 23, no. 4, pp. 385–392, 2016.

[24] P. Ghosh, C. Ghosh, and R. K. Ray, "Thermodynamics of precipitation and textural development in batch-annealed interstitial-free high-strength steels," *Acta Materialia*, vol. 58, no. 11, pp. 3842–3850, 2010.

[25] G. Tither, C. I. Garcia, M. Hua, and A. J. DeArdo, "Precipitation behavior and solute effects in interstitial-free steels," in *Physical Metallurgy of IF Steels*, pp. 293–322, Iron and Steel Institute of Japan, Tokyo, Japan, 1994.

[26] N. Yoshinaga, K. Ushioda, S. Akamatsu, and O. Akisue, "Precipitation behavior of sulfides in Ti-added ultra low-carbon steels in austenite," *ISIJ international*, vol. 34, no. 1, pp. 24–32, 1994.

[27] D. Alaoua, S. Lartigue, A. Larere, and L. Priester, "Precipitation and surface segregation in low carbon steels," *Materials Science and Engineering: A*, vol. 189, no. 1-2, pp. 155–163, 1994.

[28] M. Hua, C. I. Garcia, K. Eloot, and A. J. DeArdo, "Identification of Ti-S-C-containing multi-phase precipitates in ultra-low carbon steels by analytical electron microscopy," *ISIJ international*, vol. 37, no. 11, pp. 1129–1132, 1997.

[29] F. J. Humphreys and M. Hatherly, *Recrystallization and Related Annealing Phenomena*, Elsevier, Amsterdam, Netherlands, 2012.

[30] M. R. Barnett and J. J. Jonas, "Influence of ferrite rolling temperature on grain size and texture in annealed low C and IF steels," *ISIJ international*, vol. 37, no. 7, pp. 706–714, 1997.

[31] E. V. Pereloma, I. B. Timokhina, A. I. Nosenkov, and J. J. Jonas, "Role of Cr and P additions in the development of microstructure and texture in annealed low carbon steels," *Metalurgija*, vol. 43, no. 3, pp. 149–154, 2004.

[32] A. N. Kolmogorov, "On the statistical theory of the crystallization of metals," *Bulletin of the Academy of Sciences of the USSR, Mathematical Series*, vol. 1, pp. 355–359, 1937.

[33] J. William and R. Mehl, "Reaction kinetics in processes of nucleation and growth," *Transactions of the Metallurgical Society of AIME*, vol. 135, pp. 416–442, 1939.

[34] M. Avrami, "Kinetics of phase change. I General theory," *Journal of Chemical Physics*, vol. 7, no. 12, pp. 1103–1112, 1939.

[35] R. D. Doherty, D. A. Hughes, F. J. Humphreys et al., "Current issues in recrystallization: a review," *Materials Science and Engineering: A*, vol. 238, no. 2, pp. 219–274, 1997.

[36] R. D. Doherty, D. A. Hughes, F. J. Humphreys et al., "Current issues in recrystallization: a review," *Materials Today*, vol. 1, no. 2, pp. 14-15, 1998.

[37] T. Urabe and J. J. Jonas, "Modeling texture change during the recrystallization of an IF steel," *ISIJ International*, vol. 34, no. 5, pp. 435–442, 1994.

[38] K. Okuda and K. Seto, "Recrystallization behavior of if steel sheets immediately after hot-rolling in ferrite region," *ISIJ International*, vol. 53, no. 1, pp. 152–159, 2013.

[39] D. I. Kim, K. H. Oh, and H. C. Lee, "Statistical analysis on the development of recrystallization texture in IF steel," *Materials Science Forum*, vol. 408-412, pp. 839–844, 2002.

[40] A. A. Gazder, S. S. Hazra, and E. V. Pereloma, "Annealing behaviour and mechanical properties of severely deformed interstitial free steel," *Materials Science and Engineering: A*, vol. 530, pp. 492–503, 2011.

[41] S. S. Hazra, A. A. Gazder, and E. V. Pereloma, "Stored energy of a severely deformed interstitial free steel," *Materials Science and Engineering: A*, vol. 524, no. 1-2, pp. 158–167, 2009.

[42] A. A. Gazder, F. D. Torre, C. F. Gu, C. H. J. Davies, and E. V. Pereloma, "Microstructure and texture evolution of bcc and fcc metals subjected to equal channel angular extrusion," *Materials Science and Engineering: A*, vol. 415, no. 1-2, pp. 126–139, 2006.

[43] H. J. Frost and M. F. Ashby, *Deformation Mechanism Maps: the Plasticity and Creep of Metals and Ceramics*, Pergamon Press, Oxford, UK, 1982.

[44] A. J. Alawode and M. B. Adeyemi, "Effects of degrees of deformation and stress-relief temperatures on the mechanical properties and residual stresses of cold drawn mild steel rods," *Journal of Materials Processing Technology*, vol. 160, no. 2, pp. 112–118, 2005.

[45] O. Saray, G. Purcek, I. Karaman, T. Neindorf, and H. J. Maier, "Equal-channel angular sheet extrusion of interstitial-free (IF) steel: microstructural evolution and mechanical properties," *Materials Science and Engineering: A*, vol. 528, no. 21, pp. 6573–6583, 2011.

[46] A. Samet-Meziou, A. L. Etter, T. Baudin, and R. Penelle, "Relation between the deformation sub-structure after rolling or tension and the recrystallization mechanisms of an IF steel," *Materials Science and Engineering: A*, vol. 473, no. 1-2, pp. 342–354, 2008.

[47] T. He, Y.-d. Liu, W. Sun, and L. Zuo, "formation of nuclei with {111}," *Journal of Iron and Steel Research International*, vol. 20, no. 9, pp. 61–66, 2013.

[48] G. Purcek, O. Saray, I. Karaman, and H. J. Maier, "High strength and high ductility of ultrafine-grained, interstitial-free steel produced by ECAE and annealing," *Metallurgical and Materials Transactions A*, vol. 43, no. 6, pp. 1884–1894, 2012.

[49] A. Belyakov, Y. Kimura, and K. Tsuzaki, "Recovery and recrystallization in ferritic stainless steel after large strain deformation," *Materials Science and Engineering: A*, vol. 403, no. 1-2, pp. 249–259, 2005.

[50] X. C. Liu, H. W. Zhang, and K. Lu, "Formation of nano-laminated structure in an interstitial-free steel," *Scripta Materialia*, vol. 95, pp. 54–57, 2015.

[51] S. Tamimi, J. J. Gracio, A. B. Lopes, S. Ahzi, and F. Barlat, "Asymmetric rolling of interstitial free steel sheets: microstructural evolution and mechanical properties," *Journal of Manufacturing Processes*, vol. 31, pp. 583–592, 2018.

[52] S. P. Joshi, K. T. Ramesh, B. Q. Han, and E. J. Lavernia, "Modeling the constitutive response of bimodal metals," *Metallurgical and Materials Transactions A*, vol. 37, no. 8, p. 2397, 2006.